

Optimizing the diagnosis and assessment of chronic thromboembolic pulmonary hypertension with advancing imaging modalities

Seth Kligerman and Albert Hsiao

Cardiothoracic Imaging, University of California San Diego, La Jolla, CA, USA

Abstract

Imaging is key to nearly all aspects of chronic thromboembolic pulmonary hypertension including management for screening, assessing eligibility for pulmonary endarterectomy, and post-operative follow-up. While ventilation/perfusion scintigraphy, the gold standard technique for chronic thromboembolic pulmonary hypertension screening, can have excellent sensitivity, it can be confounded by other etiologies of pulmonary malperfusion, and does not provide structural information to guide operability assessment. Conventional computed tomography pulmonary angiography has high specificity, though findings of chronic thromboembolic pulmonary hypertension can be visually subtle and unrecognized. In addition, computed tomography pulmonary angiography can provide morphologic information to aid in pre-operative workup and assessment of other structural abnormalities. Advances in computed tomography imaging techniques, including dual-energy computed tomography and spectral-detector computed tomography, allow for improved sensitivity and specificity in detecting chronic thromboembolic pulmonary hypertension, comparable to that of ventilation/perfusion scans. Furthermore, these advanced computed tomography techniques, compared with conventional computed tomography, provide additional physiologic data from perfused blood volume maps and improved resolution to better visualize distal chronic thromboembolic pulmonary hypertension, an important consideration for balloon pulmonary angioplasty for inoperable patients. Electrocardiogram-synchronized techniques in electrocardiogram-gated computed tomography can also show further information regarding right ventricular function and structure. While the standard of care in the workup of chronic thromboembolic pulmonary hypertension includes a ventilation/perfusion scan, computed tomography pulmonary angiography, direct catheter angiography, echocardiogram, and coronary angiogram, in the future an electrocardiogram-gated dual-energy computed tomography angiography scan may enable a “one-stop” imaging study to guide diagnosis, operability assessment, and treatment decisions with less radiation exposure and cost than traditional chronic thromboembolic pulmonary hypertension imaging modalities.

Keywords

chronic thromboembolic disease pulmonary hypertension (CTEPH), imaging, dual-energy computed tomography (DECT), computed tomography pulmonary angiography (CTPA), ventilation/perfusion (V/Q) scan

Date received: 9 October 2020; accepted: 10 December 2020

Pulmonary Circulation 2021; 11(2) 1–12

DOI: 10.1177/20458940211007375

Introduction

Chronic thromboembolic embolic disease is characterized by obstruction of the pulmonary vasculature by organized thromboembolic material from major vessel thromboembolism and altered pulmonary artery remodeling secondary to a combination of abnormal angiogenesis, endothelial dysfunction, and impaired fibrinolysis.¹ When these findings lead to pulmonary hypertension, as defined by a resting mean pulmonary arterial pressure >20 mmHg and a

pulmonary vascular resistance ≥ 3 Woods units in the absence of an elevated pulmonary capillary wedge pressure,² chronic thromboembolic disease pulmonary hypertension (CTEPH) can be diagnosed (Fig. 1).³ Over time,

Corresponding author:

Seth Kligerman, Department of Radiology, University of California San Diego, 200 W Arbor Dr, #8756, San Diego, CA 92013, USA.

Email: skligerman@health.ucsd.edu



Creative Commons Non Commercial CC BY-NC: This article is distributed under the terms of the Creative Commons Attribution-NonCommercial 4.0 License (<http://www.creativecommons.org/licenses/by-nc/4.0/>) which permits non-commercial use, reproduction and distribution of the work without further permission provided the original work is attributed as specified on the SAGE and Open Access pages (<https://us.sagepub.com/en-us/nam/open-access-at-sage>).

© The Author(s) 2021
Article reuse guidelines:
sagepub.com/journals-permissions
journals.sagepub.com/home/pul



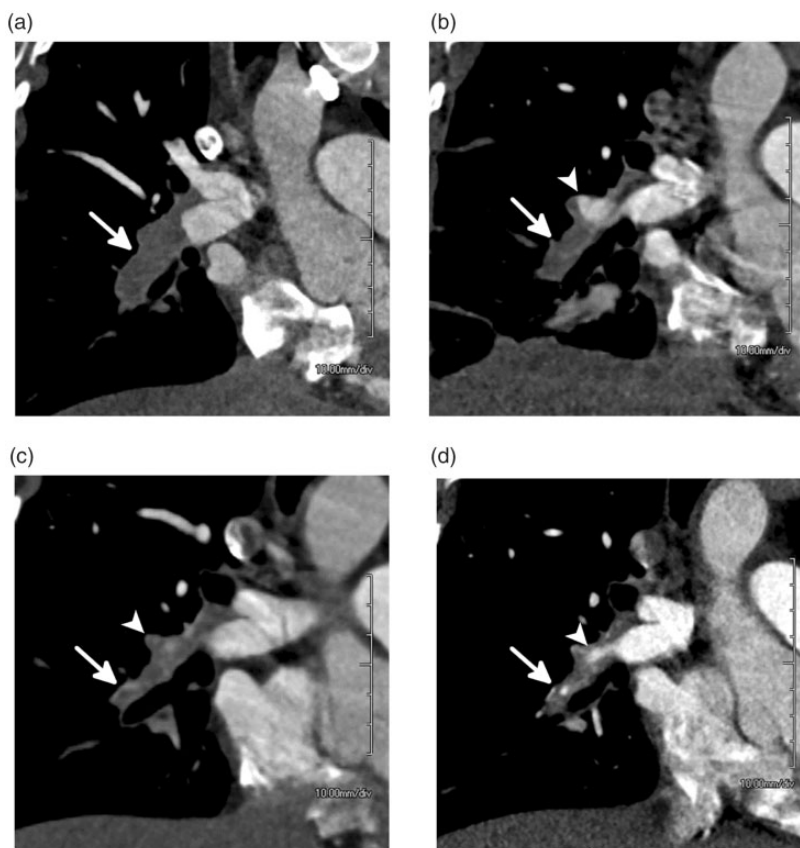


Fig. 1. Evolution of acute pulmonary embolism (PE) to chronic PE over seven months in a 33-year-old woman. (a) Coronal oblique CTPA at the time of presentation shows an acute PE filling the interlobar pulmonary artery which is expanded (white arrow). (b) CTPA one month later demonstrates dissolution of some of the clot with the proximal right middle lobar pulmonary artery now recanalized (white arrowhead). However, circumferential thrombus remains, and the vessel has begun to contract (white arrow). (c) CTPA four months after presentation shows continued contraction of the vessel (white arrow) which is filled with thrombus and scar tissue. The proximal right middle lobar pulmonary artery branch is now occluded and contracted (white arrowhead). (d) CTPA seven months after presentation shows a contracted and occluded interlobar pulmonary artery. A small amount of recanalization can be seen (white arrowhead) although the vessel remains contracted and distally occluded (white arrow).

Source: Image supplied by the authors.

elevated pulmonary pressures leads to progressive right ventricular (RV) remodeling and failure.⁴

Imaging plays a critical role in all aspects of CTEPH management from diagnosis and surgical evaluation to follow-up of patients.^{1,3,5} It is particularly important in assessing operability as pulmonary endarterectomy (PEA), the treatment of choice for CTEPH, is potentially curative. However, many patients with CTEPH are not eligible for surgery. For these patients, guidelines recommend medical therapy and, at present, the only approved and available medical therapy is riociguat.^{3,6} Balloon pulmonary angioplasty (BPA) is emerging as another important interventional treatment for these patients; it also requires imaging to assess patient suitability.^{1,3,7}

Various imaging modalities are available for assessing patients with CTEPH including ventilation/perfusion (V/Q) scintigraphy, computed tomography pulmonary angiography (CTPA), coronary angiography, direct catheter angiography, and echocardiogram.^{1,3,5} V/Q scintigraphy is

the imaging modality of choice for CTEPH screening due to its high sensitivity,^{1,3} and echocardiography has been reported as the most commonly used diagnostic modality from an international real-world survey.⁸ However, more sophisticated techniques are evolving or are already in use which may provide more information, or be easier, more accessible, or cheaper to use. This review of proceedings from our University CTEPH Symposium discusses advances in CTEPH imaging modalities, focusing on computed tomography (CT) imaging and how this compares to more traditional imaging.

V/Q scintigraphy

V/Q scintigraphy is the guideline-recommended screening method of choice for CTEPH^{1,3} and consists of ventilation and perfusion tests to detect a mismatched wedge-shaped perfusion defect, indicative of CTEPH⁵ (Fig. 2). In the ventilation scan, the patient breathes in, via a non-rebreathing

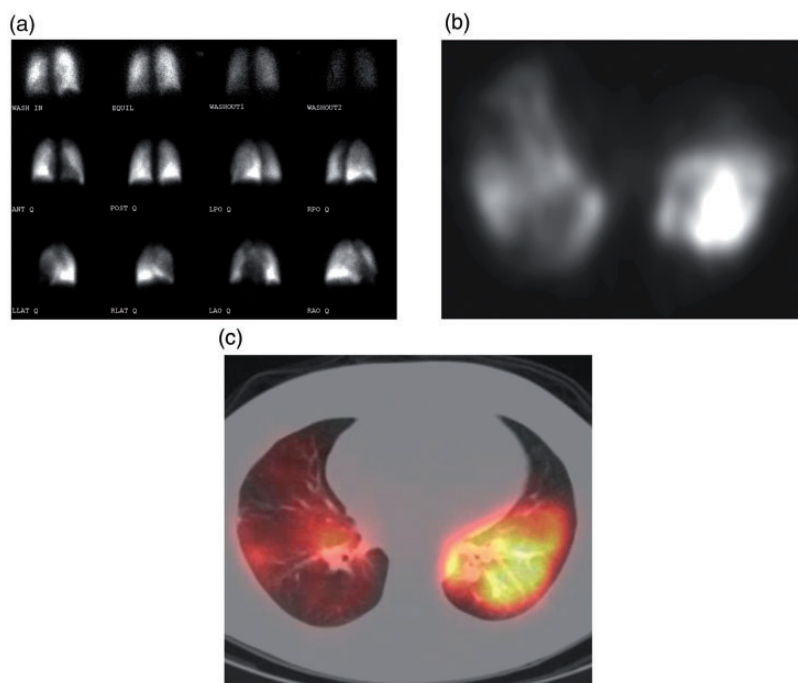


Fig. 2. V/Q scintigraphy techniques. (a) A planar V/Q scan performed in various planes on a gamma camera yields two-dimensional projections of complex three-dimensional (3-D) anatomy, akin to a radiograph. (b) A SPECT camera is a tomographic version of the gamma camera and can obtain slices through the body allowing for three-dimensional detail. (c) The data from the SPECT can be fused to a computed tomography scan to simultaneously visualize anatomy and physiology. Source: Image supplied by the authors.

mask, an aerosol of ^{99m}Tc technetium diethylenetriaminepentaacetic acid,⁹ the microparticles of which are small enough to reach distal airways. The patient is then imaged upright in three phases of initial breathing, equilibrium, and washout. In the perfusion scan, ^{99m}Tc technetium microaggregated albumin (MAA) is injected into a peripheral vein⁹ where MAA particles lodge in the pre-capillary arterioles.

V/Q 2D images are acquired from both scans using a gamma camera (Fig. 2a); however, segmental defects may be missed or underestimated due to segmental overlap and shine-through masking of adjacent lung at certain camera positions.^{7,10} Newer single-photon emission computed tomography (SPECT) cameras can overcome these limitations, providing significantly higher sensitivity 3D images^{5,11} (Fig. 2b) which can be combined with low-resolution attenuation correction CT. V/Q SPECT images can also be fused with CTPA images to provide further structural and functional information (Fig. 2c).¹⁰

Several advantages are associated with V/Q scintigraphy, primarily its high diagnostic accuracy for detecting CTEPH.⁵ A normal V/Q scan can exclude CTEPH with a sensitivity of 96–100% and a specificity of 90–95%,^{12–14} and as mismatched defects are suggestive of CTEPH but exclude pulmonary arterial hypertension (PAH), a V/Q scan is recommended by guidelines in the differential diagnosis of CTEPH and PAH.^{1,3} The ventilation scan can also provide further information about other cardiopulmonary

conditions such as heart failure and chronic obstructive lung disease.⁷ Unlike other imaging modalities, no contrast is needed in acquiring a V/Q scan, which is an advantage for patients with renal failure, due to the potential adverse reaction of contrast-induced acute kidney injury,¹⁵ and for patients with allergies to contrast.¹⁶ Lack of contrast also alleviates the need for the precise timing of the bolus. Furthermore, as required for other techniques, no breath hold is needed in obtaining the V/Q scan.

While a V/Q scan is currently the gold standard screening method for CTEPH, it provides limited, non-specific anatomical data. Additional imaging is therefore required following an abnormal V/Q scan to obtain disease morphology information to guide operability assessment and treatment decisions. Several other conditions can present with V/Q mismatch, so further imaging is also needed to determine differential diagnosis, as discussed below. Other limitations with V/Q scans can include underestimating the severity of the obstruction as radiolabeled particles can pass through partially obstructed vessels.⁵ On a practical level, it can take 30 min to acquire a V/Q scan and V/Q scans are not available at all times at most institutes or hospitals unlike CT scanners.¹⁷ Moreover, institutes or hospitals in many countries do not have V/Q scanners so other imaging modalities such as CT may be the only technique available. When using V/Q SPECT, breath-holding, which is typically used in diagnostic CT to avoid respiratory-motion

misregistration, is not feasible due to the prolonged SPECT acquisitions. It is therefore recommended that the scans are acquired during breath-holding at mid-inspiration volume or shallow breathing throughout the acquisition.¹⁰ Variability in interpreting V/Q SPECT and CT scans can also be an issue, particularly outside of expert centers.

CT imaging

Conventional CT

Conventional CT is performed using a single polychromatic X-ray beam with a range of 70–140 kV. In this energy range, differences in elemental compositions, due to unique k-edge characteristics, and photon attenuation provide inherent contrast in various tissues (e.g. fat, water, soft tissue, and bone).¹⁸ In CTPA, iodinated contrast is injected usually at a rate of 4–6 mL/s, depending on patient characteristics, into the pulmonary artery to allow for visualization of the internal anatomy of the vasculature, by exploiting the K-edge characteristics of iodine (Fig. 3).

CT is widely available in hospitals or institutes and quick to perform (<5 s). CTPA has high sensitivity (lobar 89–100%; segmental 84–91%) and specificity (lobar 96–100%; segmental 92–99%) for detecting CTEPH and is an accurate non-invasive alternative modality to conventional digital subtraction angiography (DSA).¹⁹ Furthermore, CT images also have an excellent spatial resolution of around 0.6 mm with many current imaging systems.²⁰ Unlike with V/Q scintigraphy, non-obstructive thrombi can be visualized on CT scans although it may be difficult to appreciate and can be underestimated in distal vessels (Fig. 4).⁵

Also unlike V/Q scintigraphy, CTPA can be used to assess operability as it can provide detailed structural information including endovascular thrombi, vascular wall thickness, intraluminal fibrous bands or webs, stenosis, and collateral circulation (Fig. 3).^{5,14,20} In a study assessing pre-operative workup of patients with CTEPH comparing helical CT angiography and contrast-enhanced magnetic resonance angiography of the pulmonary arteries ($n = 32$), both modalities were equally effective in detecting

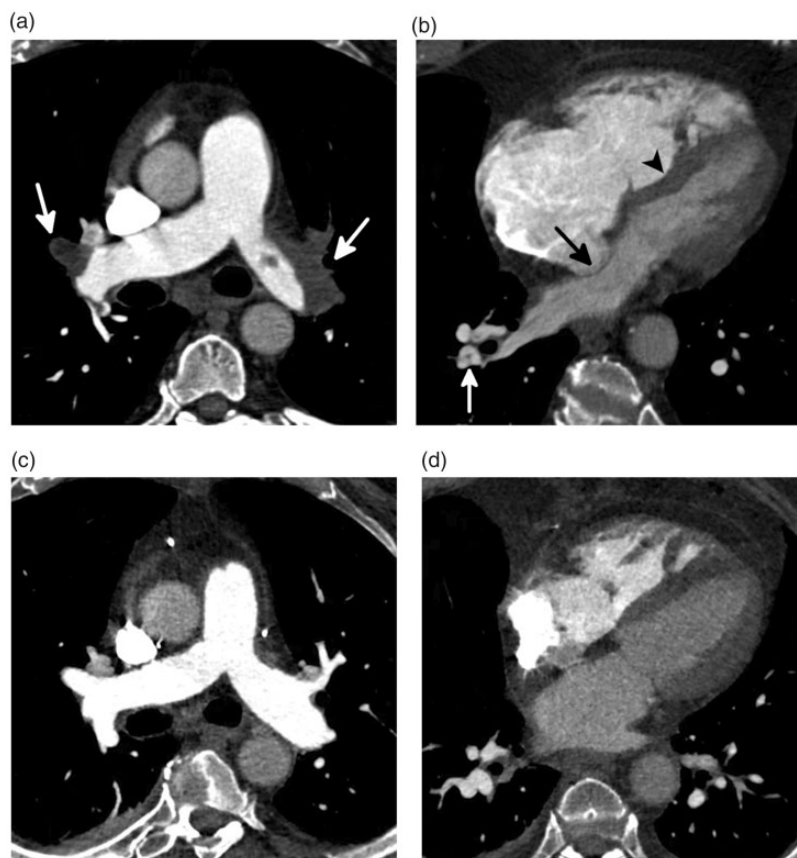


Fig. 3. CTEPH in a 57-year-old man. (a) An axial image from a CTPA through the main pulmonary arteries shows enlargement of the main pulmonary artery with occlusive thrombi bilaterally (white arrows). (b) A four-chamber image through the heart shows severe dilation and hypertrophy of the right ventricle and right atrial dilation. In addition, there is bowing of the interventricular septum with displacement of both the interventricular (black arrowhead) and interatrial (black arrow) septa to the right due to increased right ventricular and atrial pressures, respectively. A segmental web is seen in the posterior segment of the right lower lobe (white arrow). The mean pulmonary pressure was 71 mmHg before PEA. (c) An axial image through the main pulmonary artery, and (d) a four-chamber image through the heart after PEA show that the extensive thrombi have been removed. The main pulmonary artery and right heart are now normal in size, but RV hypertrophy remains. Source: Image supplied by the authors.

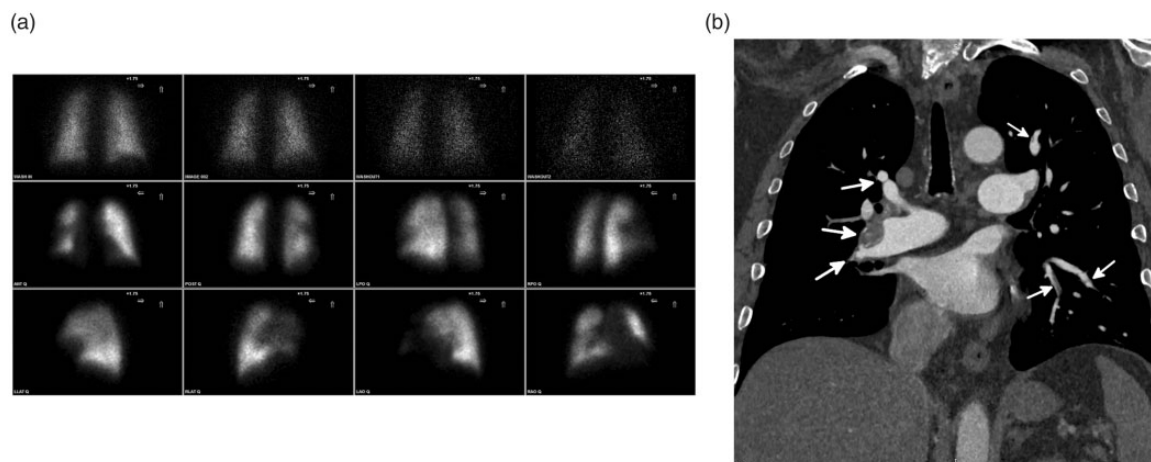


Fig. 4. Underestimation of disease burden on V/Q scan in a 53-year-old man with CTEPH. (a) A planar V/Q scan shows scattered bilateral segmental perfusion defects. (b) Coronal-oblique image from a CTPA shows numerous segmental and subsegmental areas of vascular occlusions and non-occlusive webs (white arrows). A non-obstructive layering thrombus with calcification is seen in the interlobar pulmonary artery. On V/Q scan, perfusion defects were noted in five segments. However, on CTPA, occlusive or non-occlusive disease involved the segmental and/or subsegmental vessels in all 18 segments.

Source: Image supplied by the authors.

segmental occlusions, but CT was superior in visualizing patent subsegmental arteries, intraluminal webs, and thrombotic wall thickening.²¹ Beyond the standard evaluation of the pulmonary vasculature in CTEPH, novel 3D post-processing techniques may not only provide a detailed qualitative assessment of the pulmonary arterial tree but also quantify vascular changes associated with CTEPH, including pruning and tortuosity.²²

CTPA also evaluates the lungs, enabling identification of parenchymal findings, such as a mosaic perfusion, which may help aid in the diagnosis of CTEPH. Areas of lobar, segmental, and subsegmental hypoperfusion with associated vascular attenuation due to proximal vascular occlusion are seen in over 94% of patients with CTEPH, which is significantly greater than those with other forms of pulmonary hypertension.²³ In severe cases, this is often transposed with areas of increased lung attenuation resulting from hyperperfusion of the spared regions with associated pulmonary arterial dilation (Fig. 5).²⁴ Evaluation of the lungs also allows for detection of parenchymal abnormalities, such as pulmonary fibrosis and emphysema, which, if severe, may alter treatment strategies. Finally, visualization of the entire thorax allows for one to assess for cardiovascular associations and complications of CTEPH including pulmonary artery dilation, RV and/or atrial thrombi, and cardiac structural abnormalities such as flattening of the interventricular septum, RV hypertrophy, and thickening of the outer RV wall^{14,25} (Fig. 3).

CT can provide structural and differentiating information to discriminate between several CTEPH mimics that present with perfusion defects on a V/Q scan. Examples of several CTEPH mimics that are challenging to differentiate on V/Q scan are shown in Fig. 6, including large- and medium-vessel pulmonary arteritis, pulmonary veno-occlusive disease/

pulmonary capillary hemangiomatosis, pulmonary artery sarcoma, external compression due to bronchogenic carcinoma, sarcoidosis or fibrosing mediastinitis, and congenital pulmonary vascular abnormalities.^{5,26–30}

Several disadvantages can be associated with CT as unlike V/Q scintigraphy, CTPA alone cannot exclude CTEPH.³ Also some of the practicalities of the technique can be limiting, such as the use of iodinated contrast which can be problematic for some patients as noted above, and which requires good intravenous access, ideally using the antecubital vein with an 18- or 20-gauge catheter. The timing of contrast administration is critical with CT, and scan acquisition is required at a pre-defined threshold.³¹ CT imaging also requires patient compliance as short breath holds are required to reduce respiratory motion artifacts.⁷ Finally and importantly, CT imaging requires a radiologist trained in the correct protocol, using thin slices to visualize CTEPH. Poor-quality images can be a problem in non-expert centers without the appropriate methodological rigor. Also, radiologists need to be trained and experienced in assessing imaging findings of CTEPH, as demonstrated in a study assessing original CT reports from patients with confirmed CTEPH diagnosis referred to an expert PEA center ($n=35$).³² Although most cases were visible with CT in this study, only 26% of reports identified CTEPH or signs of CTEPH, leading to a falsely low sensitivity for CT.

Electrocardiogram-gated CT

Gating techniques are used to improve resolution and reduce artifacts caused by cardiac movement. In patients with CTEPH, the use of electrocardiogram (ECG)-synchronized techniques in ECG-gated CT can provide detailed visualization of segmental and subsegmental vessels, lung parenchyma,

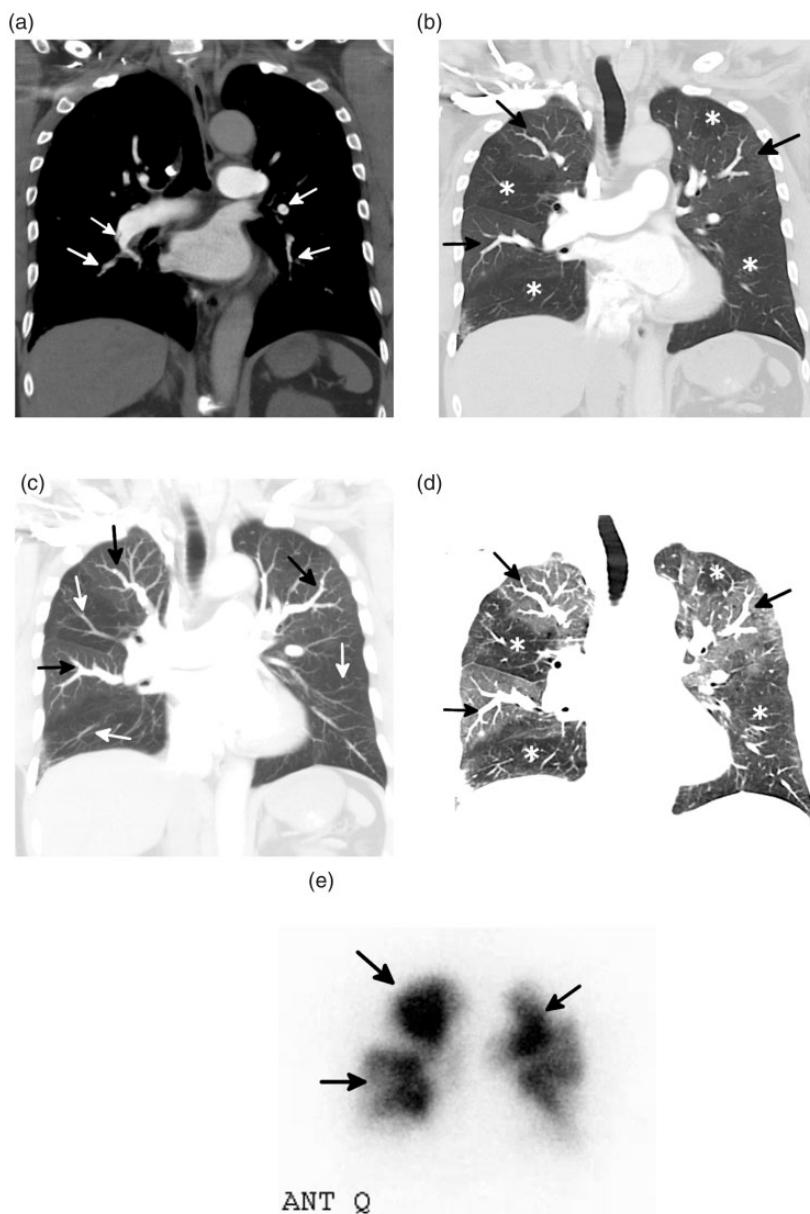


Fig. 5. Mosaic perfusion in patients with CTEPH. (a) 5 mm thick coronal CT image using a soft tissue window shows numerous areas of vascular attenuation, webs, and occlusion (arrows) due to CTEPH. (b) 5 mm thick coronal CT image in lung windows shows a prominent mosaic perfusion pattern with areas of hypoperfusion denoted by areas of decreased attenuation (asterisks) directly transposed with areas of increased perfusion denoted by areas of increased attenuation (arrows). (c) 5 mm thick maximum intensity projection coronal CT image better shows the discrepancy in vascular size with dilated pulmonary artery branches (black arrows) in the hyperperfused lungs and dramatically attenuated pulmonary artery branches (white arrows) in the hypoperfused segments. (d) 5 mm thick minimum intensity projection (MinIP) coronal CT image nicely shows the transposed areas of hypoperfusion (asterisks) and hyperperfusion (black arrows). Notice the discrepant size of the pulmonary artery branches in the hyperperfused and hypoperfused portions of the lungs. (e) Anterior projection from the perfusion portion of a V/Q scan shows that the areas of decreased (arrows) and increased Tc-99m MAA deposition on perfusion scan correlate well with the areas of hypoperfusion and hyperperfusion on CT scan.

Source: Image supplied by the authors.

and RV myocardial size and morphology, especially in the left lower lobe.^{33–35} In addition, cardiac gating can allow quantitative assessment of RV function, showing septal position and movements. This is commonly achieved on modern scanners using retrospective gating with continuous data acquisition through the cardiac cycle with considerably lower radiation

dose than historical scanners.^{7,36–38} ECG-gated CT can also be used to visualize the coronary arteries and therefore assess for significant coronary artery disease, which needs to be excluded when working up patients for PEA.³⁵ The accuracy of ECG-gated CT angiography in assessing pulmonary arteries for signs of CTEPH has been reported to be superior to

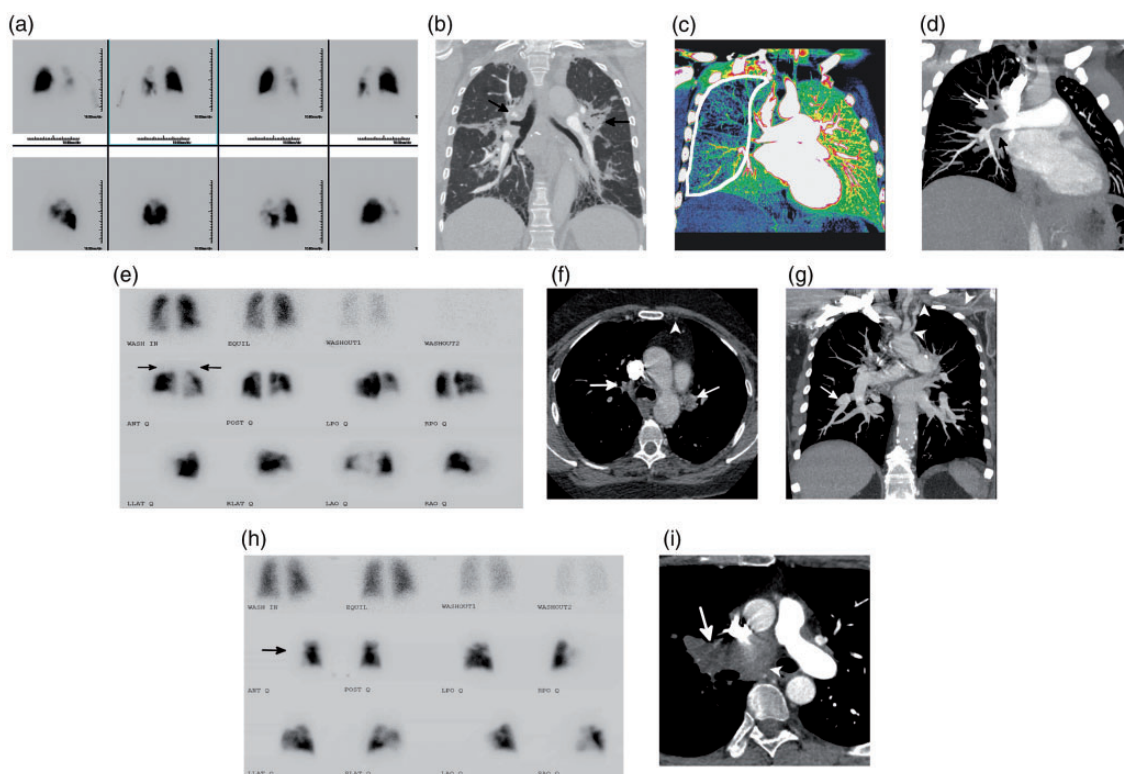


Fig. 6. Imaging examples of CTEPH mimics. (a) Planar V/Q scan with multiple perfusion defects on the left greater than the right; ventilation was normal. (b) Coronal image from a CTPA using a lung window algorithm showing compression and narrowing of the central vasculature due to conglomerate hilar soft tissue (black arrows) with associated perihilar fibrosis. A biopsy identified non-caseating granulomas consistent with sarcoid. (c) Left posterior oblique image from a dual-energy CTPA with significant decreased perfusion to the right lung (white outline). (d) Corresponding left posterior oblique maximum intensity projection image from the CTPA shows confluent right hilar soft tissue occluding the right upper lobe PA and severely narrowing the interlobar PA (white arrow). The right superior pulmonary vein is also occluded (black arrow). A biopsy identified paucicellular eosinophilic collagen, confirming the diagnosis of fibrosing mediastinitis. (e) Planar V/Q scan with bilateral upper lobe mismatches (black arrows) as well as a few additional subsegmental defects. (f) Axial CT image shows the occlusions of the upper lobe pulmonary arteries (white arrows). In addition, the left internal mammary artery is occluded (white arrowhead). (g) Coronal maximum intensity projection image with areas of branch pulmonary artery narrowing with distal aneurysmal dilation (white arrow). The left subclavian and axillary artery are diffusely narrowed and irregular with circumferential soft tissue thickening (white arrowheads). The constellation of findings is suggestive of a large-vessel vasculitis. (h) Planar V/Q scan with absence of the right lung on perfusion with normal ventilation (black arrow). (i) Axial image from a CTPA showing a large soft tissue mass filling and expanding the right pulmonary artery (white arrow) and extending into the mediastinum (white arrowhead) highly suggestive of a pulmonary artery sarcoma, which was confirmed after biopsy. Source: Image supplied by the authors.

contrast-enhanced magnetic resonance angiography and DSA. In a study assessing pulmonary arteries ($n = 24$), the sensitivity/specificity of determining CTEPH-related changes at the main/lobar and segmental levels were 100%/100% and 100%/99% with ECG-gated CT compared with 83%/99% and 88%/98% with magnetic resonance angiography and 66%/100% and 76%/100% with DSA, respectively.³⁹ In another study ($n = 44$), the sensitivity and specificity of detecting CTEPH findings were 97% at the main/lobar levels and 85% and 95% at the segmental levels, respectively, compared with DSA.⁴⁰

Dual-energy CT

The more advanced imaging technique, dual-energy CT (DECT), acquires images from two different polychromatic

X-ray beams at 80 kV and 140 kV.¹⁸ This is achieved by utilizing dual-source systems with two separate tubes and detectors or single-source systems with responsive detector scintillator materials that permit rapid kilovoltage switching and dual sampling at the low- and high-kilovoltage spectra.^{20,41} Addition of spectral CT data to conventional CTPA images has been shown to increase sensitivity and specificity of the diagnosis of CTEPH.^{14,42} DECT provides a large spectrum of different mono-energies allowing interrogation of materials based on their attenuated properties at these different energies, so changes or lack of change, i.e. when a clot is present, can be visualized. DECT can also be used to assess pulmonary perfusion in patients with CTEPH by calculating perfused blood volume (PBV) maps from iodine distribution in the lung parenchyma.^{43,44}

The ability to merge anatomical and physiologic data with DECT angiography increases the clinical utility of DECT over conventional CT by: improving detection of distal CTEPH, giving better visualization of small occlusive clots in small vessels,^{5,45} and providing more accurate information on overall pulmonary vascular reserve and parenchymal arterial perfusion.²⁰ DECT angiography can also differentiate between acute and chronic pulmonary thromboembolism.⁴⁶ Further utility from the PBV calculations with DECT includes their use in estimating the clinical severity of CTEPH as PBVs have been shown to correlate with hemodynamic measurements.^{47,48} Lung PBV analyses from DECT have also been used to assess the treatment effect of BPA with one study ($n=17$; 57 BPA sessions) reporting the sensitivity, specificity, and accuracy of detecting segmental perfusion improvements post-BPA to be 69%, 83%, and 70%, respectively.⁴⁹ Improvements in PBV after BPA were also found to be positively correlated with hemodynamics and six-minute walking distance.⁵⁰

Spectral-detector CT

Another advanced CT technique is spectral-detector CT (SDCT), which uses a poly-energetic X-ray source and a dual-layer detector. Low- and high-energy photons are simultaneously measured at the same spatial and angular location due to the nature of their respective absorption into the surface and bottom layer of the detector, resulting in less noise and improved image quality compared with conventional CT.⁵¹ Recently, a study ($n=60$) showed that SDCT had higher sensitivity (100%) and specificity (88–95%) in diagnosing CTEPH compared with conventional CT, which had a sensitivity and specificity of 79% and 85–90%, respectively.⁴² Furthermore, SDCT provided a comprehensive analysis of the pulmonary vasculature, lung parenchyma, and lung perfusion in a single test; these additional data could be valuable in helping radiologists with less experience in interpreting CT images from patients with CTEPH.⁴²

Other emerging CT techniques

Other examples of novel techniques being evaluated for use in CTEPH screening and pre-surgical planning include the addition of CT-lung subtraction iodine mapping (CT-LSIM) to conventional CTPA, which provides both high-resolution images of the pulmonary arterial vasculature and parenchymal anatomy, and functional lung perfusion information. Initial data suggest that CT-LSIM has higher diagnostic accuracy than CTPA alone;⁵² further investigation of the diagnostic performance of CT-LSIM is ongoing in the INSPIRE study.⁵³

With BPA emerging as a potential treatment option for patients with inoperable CTEPH, new techniques are also being developed and evaluated to assess pre-BPA target lesions; as yet, no imaging approach has been standardized

for BPA assessment. Several studies have shown cone-beam CT during pulmonary angiography to be useful in providing more detailed information in treatment planning for BPA, particularly in assessing subsegmental branches when compared with CTPA.^{54–56} Contrast-enhanced C-Arm CT (CACT) has been reported to provide additional findings in patients with CTEPH compared with V/Q SPECT, possibly because small intravascular webs and bands do not substantially hinder blood flow and tracer accumulation.⁵⁷ CACT has been reported to be feasible and safe as a guidance method for BPA,^{58,59} although these observations need to be validated in larger cohorts.

Approach to imaging for patients with CTEPH and future directions

Currently, the imaging workup for patients with CTEPH includes various invasive and non-invasive studies across multiple modalities including V/Q scan, echocardiogram, digital subtraction pulmonary angiography, CTPA, and coronary artery catheterization.⁶ When considering the use of new emerging imaging modalities such as CT-based techniques in CTEPH management, several aspects, including diagnostic accuracy, detail of anatomical information, and radiation exposure, should be considered in relation to other imaging techniques, particularly V/Q scintigraphy.

Several studies have demonstrated that CT, particularly DECT, imaging provides high sensitivity and specificity in detecting CTEPH, comparable with V/Q scintigraphy. A meta-analysis of 11 studies assessing the diagnostic accuracy of CT, using V/Q scanning or DSA as a reference standard, reported a pooled sensitivity of 88%, 95%, and 88% for total arteries, main and lobar arteries, and segmental arteries, respectively, and a pooled specificity of 90%, 96%, and 89%, respectively.⁴⁵ Similar sensitivities and specificities comparing diagnostic accuracy between DECT perfusion and V/Q scans have been reported. In 80 patients undergoing DECT perfusion and V/Q scanning, sensitivity for CTEPH diagnosis was 97% for both modalities and specificity was 86% and 100%, respectively.⁶⁰ However, in this study, the anatomical information from DECT enabled the false positives and negatives to be correctly reclassified, so the sensitivity and specificity for DECT perfusion were 100%. In another study ($n=51$), agreement between DECT PBV images and V/Q scans was good, with DECT showing a sensitivity and specificity in detecting perfusion defects of 96% and 76%, respectively.⁶¹ At a segmental/vessel level, DECT perfusion has higher diagnostic accuracy than CTPA,^{45,62} which with the evolution of BPA is an important consideration. In a study with 40 patients where DECT perfusion showed a moderate agreement with V/Q scans, only a fair to slight agreement was reported with CTPA.⁶² Importantly, as discussed above, CTPA and DECT perfusion, unlike V/Q scintigraphy, also provide detailed anatomical information which is required to

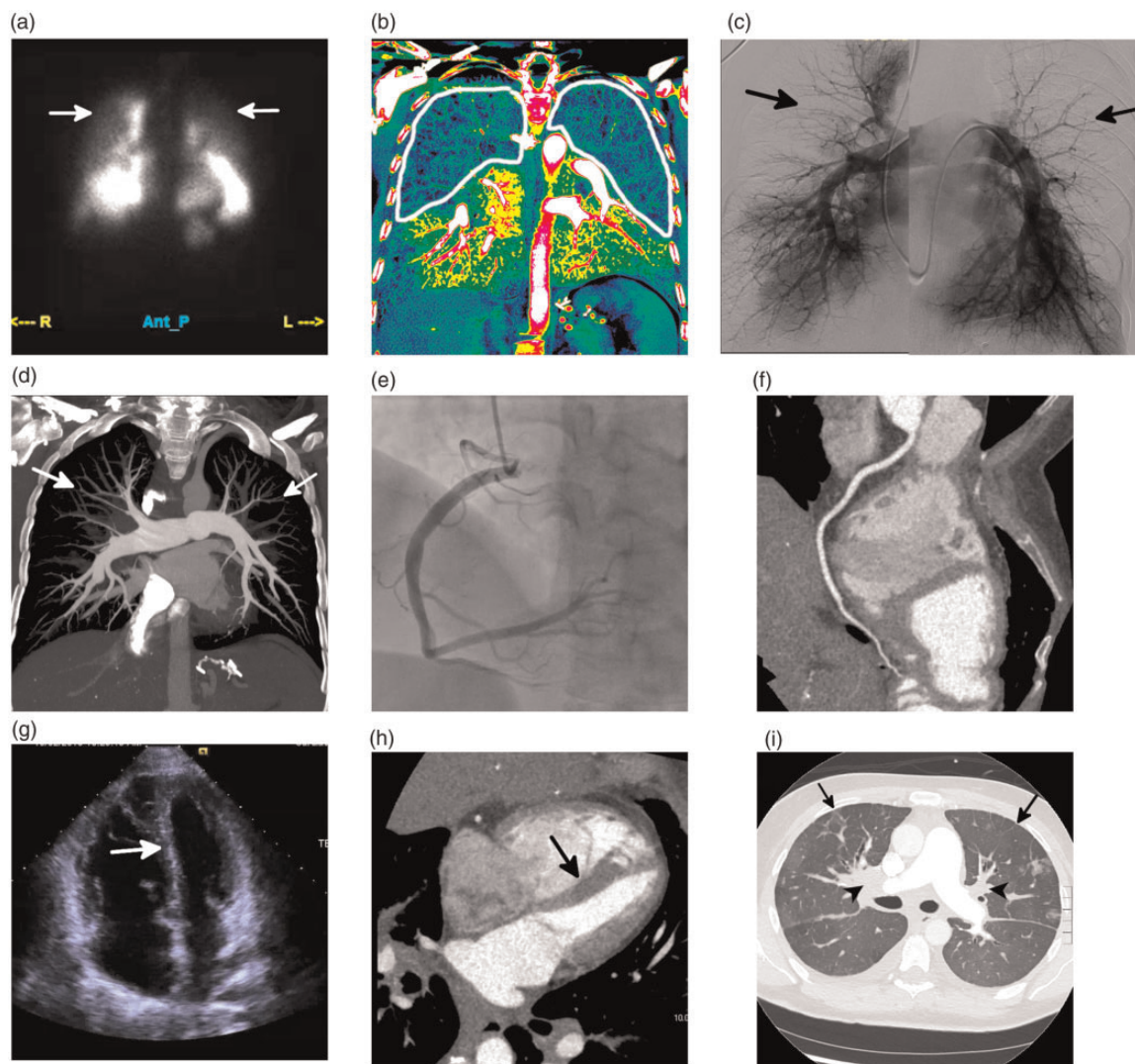


Fig. 7. Side-by-side comparison of a traditional imaging workup for CTEPH, using multiple modalities, and a novel approach with a retrospectively gated coronary CT angiography (CTA) and dual-energy CT pulmonary angiography (DE-CTPA) acquired as a single exam. (a and b) An anterior image from a planar V/Q scan (a) shows decreased upper lung perfusion (white arrows), and coronal iodine map from the DE-CTPA study (b) shows decreased upper lobe and peripheral perfusion bilaterally (white outline). (c and d) Fused image of DSA (c) and a 20 mm thick maximum intensity projection from the DE-CTPA (d) both show peripheral pruning of the vasculature (arrows, c and d) but no evidence of chronic thromboembolic disease. (e and f) Images of the right coronary artery from a coronary catheterization (e) and a multiplanar reformat from the coronary CTA (f) both show that the vessel is free of disease. (g and h) Four-chamber image from an echocardiogram (g), and retrospectively gated coronary CTA (h) both show right ventricular hypertrophy and inversion of the interventricular septum (arrows, g and h). (i) An axial image of the lung from the single CTPA/coronary CTA study shows confluent perihilar soft tissue (black arrowheads) with prominent septal thickening (black arrows). Left ventricular function on both echocardiography and CTA was normal. The constellation of findings is highly suggestive of pulmonary veno-occlusive disease and not CTEPH. Continued medical management was recommended. This combined dual-energy CTPA and coronary CTA exam has both a lower cost and radiation dose compared with the traditional workup, which includes a V/Q scan, DSA, CTA, coronary angiogram, and echocardiogram. However, further studies are needed to assess the feasibility of this protocol. Source: Image supplied by the authors.

inform operability assessment; additional imaging would therefore not be needed if CT imaging was used in the initial diagnostic workup.

Where possible, radiation exposure in CTEPH imaging should be limited and strategies put in place to reduce exposure.⁶³ The cumulative radiation exposure in diagnosing a patient with CTEPH using the traditional imaging pathway

can be high, i.e. V/Q scan (0.9–5.9 mSv), digital subtraction pulmonary angiogram (6.0–9.0 mSv), coronary artery catheterization (2–20 mSv), and CTPA (1.4–10 mSv).^{63–68} While CTPA previously used higher radiation doses than V/Q scans,¹⁷ modern CT scanners with newer iterative and model-based reconstruction techniques now use similar radiation doses to V/Q scans.^{68–71} In a meta-analysis

assessing the use of CTPA or V/Q scans in pregnant women to diagnose pulmonary embolism, no significant differences were observed in the radiation dose received; the mean maternal effective dose ranged from 0.2 to 9.7 mSv with CT and 0.9 to 5.0 mSv with a V/Q scan.⁶⁵

A novel approach to incorporate all the above factors should be considered, whereby one imaging study is performed that can provide qualitative and quantitative assessment of pulmonary perfusion, high spatial resolution assessment of the pulmonary arteries and coronary arteries, and morphologic and quantitative assessment of the heart, all with lower radiation exposure and overall cost. Such an approach could include a single ECG-gated dual-energy CTPA and coronary CT angiography exam (Fig. 7). The radiation exposure from this single acquisition would be approximately 6–10 mSv, much lower than the cumulative radiation exposure of traditional imaging. Furthermore, this approach would be associated with significant cost benefits. At the authors' institution, the cost of a V/Q scan, selective bilateral pulmonary artery angiography, coronary angiography, and echocardiogram, excluding additional costs of anesthesia, would be approximately \$24,000. This represents an eight-fold greater cost compared with a gated CT angiography of the chest, which costs approximately \$3000.⁷² However, while this approach may seem promising, it would need to be researched and validated before it could potentially replace the traditional imaging approach to CTEPH. Additionally, implementation on a broad scale would be limited by access to DECT perfusion in some areas, and further initiatives may be needed to standardize data collection and interpretation techniques and to educate radiologists on optimizing these techniques.

Conclusions

V/Q scintigraphy has excellent diagnostic accuracy and is the guideline-recommended imaging of choice for exclusion of CTEPH. However, several advances in CT imaging have improved its iodine contrast and resolution, enabling simultaneous detailed evaluation of morphology, lung perfusion, disease severity, and RV function. Further studies are needed to verify the appropriate use of these new techniques in routine clinical practice to optimize CTEPH management.

Acknowledgments

Medical writing services provided by Richard Murphy PhD of Adelphi Communications Ltd, Macclesfield, UK.

Author contributions

This article is based on a presentation by Professor Kligerman at the University of California San Diego CTEPH Symposium, 15–16 November 2019, with additional material by Professor Kligerman and Professor Hsiao. Both authors reviewed each draft, supplied all images, and approved the final draft for submission.

Conflict of interest

The author(s) declared the following potential conflicts of interest with respect to the research, authorship, and/or publication of this article: Professor Kligerman has no conflicts of interest. Professor Hsiao reports research grants from GE Healthcare, is a co-founder of, shareholder in, and receives consulting fees from Arterys, research grants from Bayer AG, and intellectual property rights from Stanford University and UC San Diego, outside the submitted work.

Ethical approval

Not applicable (no patient interventions were performed for the purposes of this article).

Guarantor

Professor Kligerman is the guarantor of the accuracy of the data presented in this review.

Funding

The authors disclosed receipt of the following financial support for the research, authorship, and/or publication of this article: This study was funded by Bayer US LLC, Whippany, NJ, USA.

References

1. Kim NH, Delcroix M, Jais X, et al. Chronic thromboembolic pulmonary hypertension. *Eur Respir J* 2019; 53.
2. Simonneau G, Montani D, Celermajer DS, et al. Haemodynamic definitions and updated clinical classification of pulmonary hypertension. *Eur Respir J* 2019; 53: 1801913.
3. Galiè N, Humbert M, Vachiery JL, et al. 2015 ESC/ERS guidelines for the diagnosis and treatment of pulmonary hypertension: the joint task force for the diagnosis and treatment of pulmonary hypertension of the European Society of Cardiology (ESC) and the European Respiratory Society (ERS); endorsed by: Association for European Paediatric and Congenital Cardiology (AEPC), International Society for Heart and Lung Transplantation (ISHLT). *Eur Respir J* 2015; 46: 903–975.
4. Delcroix M, Vonk Noordegraaf A, Fadel E, et al. Vascular and right ventricular remodelling in chronic thromboembolic pulmonary hypertension. *Eur Respir J* 2013; 41: 224–232.
5. Gopalan D, Blanchard D and Auger WR. Diagnostic evaluation of chronic thromboembolic pulmonary hypertension. *Ann Am Thorac Soc* 2016; 13 Suppl 3: S222–S239.
6. Mahmud E, Madani MM, Kim NH, et al. Chronic thromboembolic pulmonary hypertension: evolving therapeutic approaches for operable and inoperable disease. *J Am Coll Cardiol* 2018; 71: 2468–2486.
7. Gopalan D, Delcroix M and Held M. Diagnosis of chronic thromboembolic pulmonary hypertension. *Eur Respir Rev* 2017; 26: 160108.
8. Gall H, Preston IR, Hinzmann B, et al. An international physician survey of chronic thromboembolic pulmonary hypertension management. *Pulm Circ* 2016; 6: 472–482.
9. Ruggiero A and Sreaton NJ. Imaging of acute and chronic thromboembolic disease: state of the art. *Clin Radiol* 2017; 72: 375–388.
10. Roach PJ, Schembri GP and Bailey DL. V/Q scanning using SPECT and SPECT/CT. *J Nucl Med* 2013; 54: 1588–1596.

11. Soler X, Hoh CK, Test VJ, et al. Single photon emission computed tomography in chronic thromboembolic pulmonary hypertension. *Respirology* 2011; 16: 131–137.
12. He J, Fang W, Lv B, et al. Diagnosis of chronic thromboembolic pulmonary hypertension: comparison of ventilation/perfusion scanning and multidetector computed tomography pulmonary angiography with pulmonary angiography. *Nucl Med Commun* 2012; 33: 459–463.
13. Tunariu N, Gibbs SJ, Win Z, et al. Ventilation-perfusion scintigraphy is more sensitive than multidetector CTPA in detecting chronic thromboembolic pulmonary disease as a treatable cause of pulmonary hypertension. *J Nucl Med* 2007; 48: 680–684.
14. Kiely DG, Levin D, Hassoun P, et al. Statement on imaging and pulmonary hypertension from the Pulmonary Vascular Research Institute (PVRI). *Pulm Circ* 2019; 9: 1–32.
15. Fahling M, Seeliger E, Patzak A, et al. Understanding and preventing contrast-induced acute kidney injury. *Nat Rev Nephrol* 2017; 13: 169–180.
16. Singh J and Daftary A. Iodinated contrast media and their adverse reactions. *J Nucl Med Technol* 2008; 36: 69–74; quiz 76–77.
17. Freeman LM. Don't bury the V/Q scan: it's as good as multidetector CT angiograms with a lot less radiation exposure. *J Nucl Med* 2008; 49: 5–8.
18. Patino M, Prochowski A, Agrawal MD, et al. Material separation using dual-energy CT: current and emerging applications. *Radiographics* 2016; 36: 1087–1105.
19. Reichelt A, Hoepfer MM, Galanski M, et al. Chronic thromboembolic pulmonary hypertension: evaluation with 64-detector row CT versus digital subtraction angiography. *Eur J Radiol* 2009; 71: 49–54.
20. Ameli-Renani S, Rahman F, Nair A, et al. Dual-energy CT for imaging of pulmonary hypertension: challenges and opportunities. *Radiographics* 2014; 34: 1769–1790.
21. Ley S, Kauczor HU, Heussel CP, et al. Value of contrast-enhanced MR angiography and helical CT angiography in chronic thromboembolic pulmonary hypertension. *Eur Radiol* 2003; 13: 2365–2371.
22. Rahaghi FN, Ross JC, Agarwal M, et al. Pulmonary vascular morphology as an imaging biomarker in chronic thromboembolic pulmonary hypertension. *Pulm Circ* 2016; 6: 70–81.
23. Grosse A, Grosse C and Lang IM. Distinguishing chronic thromboembolic pulmonary hypertension from other causes of pulmonary hypertension using CT. *AJR Am J Roentgenol* 2017; 209: 1228–1238.
24. Kligerman SJ, Henry T, Lin CT, et al. Mosaic attenuation: etiology, methods of differentiation, and pitfalls. *Radiographics* 2015; 35: 1360–1380.
25. Dogan H, de Roos A, Geleijns J, et al. The role of computed tomography in the diagnosis of acute and chronic pulmonary embolism. *Diagn Interv Radiol* 2015; 21: 307–316.
26. Ali N, Clarke L, MacKenzie Ross RV, et al. Pulmonary vasculitis mimicking chronic thromboembolic disease. *BMJ Case Rep* 2019; 12: e228409.
27. Bailey CL, Channick RN, Auger WR, et al. "High probability" perfusion lung scans in pulmonary venoocclusive disease. *Am J Respir Crit Care Med* 2000; 162: 1974–1978.
28. Kauczor HU, Schwickert HC, Mayer E, et al. Pulmonary artery sarcoma mimicking chronic thromboembolic disease: computed tomography and magnetic resonance imaging findings. *Cardiovasc Intervent Radiol* 1994; 17: 185–189.
29. Kerr KM, Auger WR, Fedullo PF, et al. Large vessel pulmonary arteritis mimicking chronic thromboembolic disease. *Am J Respir Crit Care Med* 1995; 152: 367–373.
30. Narechania S, Renapurkar R and Heresi GA. Mimickers of chronic thromboembolic pulmonary hypertension on imaging tests: a review. *Pulm Circ* 2020; 10: 2045894019882620.
31. Lewis G, Hoey ET, Reynolds JH, et al. Multi-detector CT assessment in pulmonary hypertension: techniques, systematic approach to interpretation and key findings. *Quant Imaging Med Surg* 2015; 5: 423–432.
32. Rogberg AN, Gopalan D, Westerlund E, et al. Do radiologists detect chronic thromboembolic disease on computed tomography? *Acta Radiol* 2019; 60: 1576–1583.
33. Desjardins B and Kazerooni EA. ECG-gated cardiac CT. *AJR Am J Roentgenol* 2004; 182: 993–1010.
34. Ozawa K, Funabashi N, Takaoka H, et al. Detection of right ventricular myocardial fibrosis using quantitative CT attenuation of the right ventricular myocardium in the late phase on 320 slice CT in subjects with pulmonary hypertension. *Int J Cardiol* 2017; 228: 165–168.
35. Wirth G, Bruggemann K, Bostel T, et al. Chronic thromboembolic pulmonary hypertension (CTEPH) - potential role of multidetector-row CT (MD-CT) and MR imaging in the diagnosis and differential diagnosis of the disease. *Rofa* 2014; 186: 751–761.
36. Kang EJ. Clinical applications of wide-detector CT scanners for cardiothoracic imaging: an update. *Korean J Radiol* 2019; 20: 1583–1596.
37. Hedgire SS, Baliyan V, Ghoshhajra BB, et al. Recent advances in cardiac computed tomography dose reduction strategies: a review of scientific evidence and technical developments. *J Med Imaging (Bellingham)* 2017; 4: 031211.
38. Patel N, Li D, Nakanishi R, et al. Comparison of whole heart computed tomography scanners for image quality lower radiation dosing in coronary computed tomography angiography: the CONVERGE registry. *Acad Radiol* 2019; 26: 1443–1449.
39. Ley S, Ley-Zaporozhan J, Pitton MB, et al. Diagnostic performance of state-of-the-art imaging techniques for morphological assessment of vascular abnormalities in patients with chronic thromboembolic pulmonary hypertension (CTEPH). *Eur Radiol* 2012; 22: 607–616.
40. Sugiura T, Tanabe N, Matsuura Y, et al. Role of 320-slice CT imaging in the diagnostic workup of patients with chronic thromboembolic pulmonary hypertension. *Chest* 2013; 143: 1070–1077.
41. McCollough CH, Leng S, Yu L, et al. Dual- and multi-energy CT: principles, technical approaches, and clinical applications. *Radiology* 2015; 276: 637–653.
42. Kroger JR, Gerhardt F, Dumitrescu D, et al. Diagnosis of pulmonary hypertension using spectral-detector CT. *Int J Cardiol* 2019; 285: 80–85.
43. Hoey ET, Mirsadraee S, Pepke-Zaba J, et al. Dual-energy CT angiography for assessment of regional pulmonary perfusion in patients with chronic thromboembolic pulmonary hypertension: initial experience. *AJR Am J Roentgenol* 2011; 196: 524–532.
44. Renard B, Remy-Jardin M, Santangelo T, et al. Dual-energy CT angiography of chronic thromboembolic disease: can it help recognize links between the severity of pulmonary arterial obstruction and perfusion defects? *Eur J Radiol* 2011; 79: 467–472.

45. Dong C, Zhou M, Liu D, et al. Diagnostic accuracy of computed tomography for chronic thromboembolic pulmonary hypertension: a systematic review and meta-analysis. *PLoS One* 2015; 10: e0126985.
46. Kim SS, Hur J, Kim YJ, et al. Dual-energy CT for differentiating acute and chronic pulmonary thromboembolism: an initial experience. *Int J Cardiovasc Imaging* 2014; 30 Suppl 2: 113–120.
47. Takagi H, Ota H, Sugimura K, et al. Dual-energy CT to estimate clinical severity of chronic thromboembolic pulmonary hypertension: comparison with invasive right heart catheterization. *Eur J Radiol* 2016; 85: 1574–1580.
48. Meinel FG, Graef A, Thierfelder KM, et al. Automated quantification of pulmonary perfused blood volume by dual-energy CTPA in chronic thromboembolic pulmonary hypertension. *Rofo* 2014; 186: 151–156.
49. Koike H, Sueyoshi E, Sakamoto I, et al. Comparative clinical and predictive value of lung perfusion blood volume CT, lung perfusion SPECT and catheter pulmonary angiography images in patients with chronic thromboembolic pulmonary hypertension before and after balloon pulmonary angioplasty. *Eur Radiol* 2018; 28: 5091–5099.
50. Koike H, Sueyoshi E, Sakamoto I, et al. Quantification of lung perfusion blood volume (lung PBV) by dual-energy CT in patients with chronic thromboembolic pulmonary hypertension (CTEPH) before and after balloon pulmonary angioplasty (BPA): preliminary results. *Eur J Radiol* 2016; 85: 1607–1612.
51. Doerner J, Wybranski C, Byrtus J, et al. Intra-individual comparison between abdominal virtual mono-energetic spectral and conventional images using a novel spectral detector CT. *PLoS One* 2017; 12: e0183759.
52. Tamura M, Yamada Y, Kawakami T, et al. Diagnostic accuracy of lung subtraction iodine mapping CT for the evaluation of pulmonary perfusion in patients with chronic thromboembolic pulmonary hypertension: correlation with perfusion SPECT/CT. *Int J Cardiol* 2017; 243: 538–543.
53. Shahin Y, Johns C, Karunasaagarar K, et al. IodiNe Subtraction mapping in the diagnosis of pulmonary chronic thromboembolic disease (INSPIRE): rationale and methodology of a cross-sectional observational diagnostic study. *Contemp Clin Trials Commun* 2019; 15: 100417.
54. Fukuda T, Ogo T, Nakanishi N, et al. Evaluation of organized thrombus in distal pulmonary arteries in patients with chronic thromboembolic pulmonary hypertension using cone-beam computed tomography. *Jpn J Radiol* 2016; 34: 423–431.
55. Ogo T, Fukuda T, Tsuji A, et al. Efficacy and safety of balloon pulmonary angioplasty for chronic thromboembolic pulmonary hypertension guided by cone-beam computed tomography and electrocardiogram-gated area detector computed tomography. *Eur J Radiol* 2017; 89: 270–276.
56. Sugiyama M, Fukuda T, Sanda Y, et al. Organized thrombus in pulmonary arteries in patients with chronic thromboembolic pulmonary hypertension; imaging with cone beam computed tomography. *Jpn J Radiol* 2014; 32: 375–382.
57. Hinrichs JB, Werncke T, Kaireit T, et al. C-Arm computed tomography adds diagnostic information in patients with chronic thromboembolic pulmonary hypertension and a positive V/Q SPECT. *Rofo* 2017; 189: 49–56.
58. Hinrichs JB, Renne J, Hoepfer MM, et al. Balloon pulmonary angioplasty: applicability of C-Arm CT for procedure guidance. *Eur Radiol* 2016; 26: 4064–4071.
59. Maschke SK, Hinrichs JB, Renne J, et al. C-Arm computed tomography (CACT)-guided balloon pulmonary angioplasty (BPA): evaluation of patient safety and peri- and post-procedural complications. *Eur Radiol* 2019; 29: 1276–1284.
60. Masy M, Giordano J, Petyt G, et al. Dual-energy CT (DECT) lung perfusion in pulmonary hypertension: concordance rate with V/Q scintigraphy in diagnosing chronic thromboembolic pulmonary hypertension (CTEPH). *Eur Radiol* 2018; 28: 5100–5110.
61. Nakazawa T, Watanabe Y, Hori Y, et al. Lung perfused blood volume images with dual-energy computed tomography for chronic thromboembolic pulmonary hypertension: correlation to scintigraphy with single-photon emission computed tomography. *J Comput Assist Tomogr* 2011; 35: 590–595.
62. Dournes G, Verdier D, Montaudon M, et al. Dual-energy CT perfusion and angiography in chronic thromboembolic pulmonary hypertension: diagnostic accuracy and concordance with radionuclide scintigraphy. *Eur Radiol* 2014; 24: 42–51.
63. Einstein AJ, Berman DS, Min JK, et al. Patient-centered imaging: shared decision making for cardiac imaging procedures with exposure to ionizing radiation. *J Am Coll Cardiol* 2014; 63: 1480–1489.
64. Carpeggiani C, Picano E, Brambilla M, et al. Variability of radiation doses of cardiac diagnostic imaging tests: the RADIO-EVINCI study (RADIationOse subproject of the EVINCI study). *BMC Cardiovasc Disord* 2017; 17: 63.
65. Tromeur C, van der Pol LM, Le Roux P-Y, et al. Computed tomography pulmonary angiography versus ventilation-perfusion lung scanning for diagnosing pulmonary embolism during pregnancy: a systematic review and meta-analysis. *Haematologica* 2019; 104: 176–188.
66. White C. Radiation dose considerations in the chest. *Appl Radiol*, www.appliedradiology.com/articles/radiation-dose-considerations-in-the-chest (2009, accessed 26 March 2021).
67. Cohen SL, Wang JJ, Chan N, et al. Predictors of radiation dose for CT pulmonary angiography in pregnancy across a multihospital integrated healthcare network. *Eur J Radiol* 2019; 121: 108721.
68. Lenga L, Trapp F, Albrecht MH, et al. Single- and dual-energy CT pulmonary angiography using second- and third-generation dual-source CT systems: comparison of radiation dose and image quality. *Eur Radiol* 2019; 29: 4603–4612.
69. Leithner D, Gruber-Rouh T, Beeres M, et al. 90-kVp low-tube-voltage CT pulmonary angiography in combination with advanced modeled iterative reconstruction algorithm: effects on radiation dose, image quality and diagnostic accuracy for the detection of pulmonary embolism. *Br J Radiol* 2018; 91: 20180269.
70. Sauter A, Koehler T, Brendel B, et al. CT pulmonary angiography: dose reduction via a next generation iterative reconstruction algorithm. *Acta Radiol* 2019; 60: 478–487.
71. Boos J, Kropil P, Lanzman RS, et al. CT pulmonary angiography: simultaneous low-pitch dual-source acquisition mode with 70 kVp and 40 ml of contrast medium and comparison with high-pitch spiral dual-source acquisition with automated tube potential selection. *Br J Radiol* 2016; 89: 20151059.
72. UC San Diego Health. Billing & insurance, <https://health.ucsd.edu/patients/billing/standard-charges/Pages/default.aspx> (accessed 1 June 2020).